


## Original article

# Propagation of pressure drop in coalbed methane reservoir during drainage stage

Ding Jia<sup>1,2</sup>, Yongkai Qiu<sup>1,2</sup>, Chong Li<sup>1,2</sup>, Yidong Cai<sup>1,2</sup>\*

<sup>1</sup> School of Energy Resources, China University of Geosciences, Beijing 100083, P. R. China

<sup>2</sup> Coal Reservoir Laboratory of National Engineering Research Center of CBM Development & Utilization, China University of Geosciences, Beijing 100083, P. R. China

(Received November 14, 2019; revised December 4, 2019; accepted December 4, 2019; available online December 6, 2019)

### Citation:

Jia, D., Qiu, Y., Li, C., Cai, Y. Propagation of pressure drop in coalbed methane reservoir during drainage stage. *Advances in Geo-Energy Research*, 2019, 3(4): 387-395, doi: 10.26804/ager.2019.04.06.

### Corresponding author:

\*E-mail: yidong.cai@cugb.edu.cn

### Keywords:

Drainage stage  
coalbed methane  
multi-field coupling  
pressure drop propagation  
Zhengzhuang block

### Abstract:

Numerical simulation was employed to investigate the propagation speed of pressure drop at the drainage stage in coalbed methane (CBM) reservoirs. A seepage model of single-phase water in CBM reservoirs was generated with the parameter from CBM well ZS39 in the Zhengzhuang block of the southern Qinshui Basin. The effects of stress sensitivity and reservoir properties on the pressure drop propagation process were analysed. Moreover the pressure drop funnel scale index was introduced to quantitatively characterize the propagation process. The results indicate that stress sensitivity cause the permeability form the permeability drop funnel, which is consistent with the shape of the pressure drop funnel. Under the constant bottom pressure, the propagation speed of the funnel will gradually decrease in both longitudinal and lateral direction. And the overall propagation speed rapidly increases first and then gradually decreases. In the scenario of steady decrease in the bottomhole pressure, the pressure drop speed shows an increasing trend in the longitudinal direction, and a decreasing trend in the lateral direction. The overall propagation speed of the pressure drop funnel increases all along. The reservoir pressure drop is positively correlated with the initial porosity, the initial permeability and the elastic modulus. For Poisson ratio, when the ratio is small, the reservoir pressure drop has a negative correlation. As Poisson ratio increases over 0.35, a positive correlation exists. It was found from the sensitivity analysis of reservoir pressure drop that petrophysical parameters have strong sensitivity to pressure drop, especially for permeability. Therefore, this work may provide insights into the CBM reservoir properties, and thus will be favorable for improving CBM recovery.

## 1. Introduction

Coalbed methane (CBM) is a kind of clean energy. The processes of CBM exploitation include the single water drainage phase, gas-water phase and single gas phase. The gas desorption in CBM reservoir needs to reduce the reservoir pressure to the critical desorption pressure. With the relationship between the reservoir pressure and the critical desorption pressure of coal seam, the production of water saturated CBM wells can be divided into two stages, one for drainage stage and another for gas production stage. Drainage and depressurization are the main ways to reduce the reservoir pressure (Liu and Lou, 2004; Sang and Xu, 2010; Dejam et al., 2018). Therefore, understanding the propagation of pressure drop funnel and the controlling factors is of great significance.

In the process of drainage and depressurization, with the decrease of reservoir pressure, the same reservoir pressure

point will form a curved surface from the wellbore to the supply edge similar to the funnel, i.e. pressure drop funnel (Clarkson and Qanbari, 2016; Mendhe et al., 2016). The top of the pressure drop funnel is relatively flat, and it suddenly becomes steep near the wellbore. The bottom of the funnel is in the shape of a slender cone, and the fluid energy is mainly consumed near the well (Clarkson, 2009; Wang et al., 2013). In order to achieve the best mining effect, it is necessary to expand the propagation area of pressure drop funnel as much as possible (Palmer and Mansoori, 1998; Ide et al., 2010). The ratio of longitudinal pressure drop to drainage radius was used to characterize the strength of CBM reservoir lamination. The smaller the value is, the more obvious the horizontal propagation of the pressure drop funnel is. And the larger the value is, the more obvious the longitudinal deepening is (Majdi et al., 2016; Wang et al., 2019). Four different types of pressure drop funnel models of logarithmic function,



<https://doi.org/10.26804/ager.2019.04.06>.

2207-9963 © The Author(s) 2019. Published with open access at Ausasia Science and Technology Press on behalf of the Division of Porous Flow, Hubei Province Society of Rock Mechanics and Engineering.

linear function, parabola function and elliptic function can be used to study the effect of pressure drop funnel shapes on CBM well productivity. Under the same drop funnels radius, the desorption radius and effective desorption radius of logarithmic, linear, paraboloid and elliptic function models were expanded successively (Hu et al., 2019).

The water saturation was deemed as a constant during the full CBM well production life. The material balance equation can be utilized to obtain reserves and drainage area of CBM wells. Previous research shows that the propagation process of the coal bed methane reservoir pressure could be divided into two stages. The first stage would be before the pressure propagate to the boundary of the reservoir and the second stage would be the pressure propagate beyond the boundary of the reservoir (Connell, 2016). If the rate of drainage pressure reduction is too fast, there will be stress sensitive effect and speed sensitive formation, and may enter the gas-water two-phase flow stage too early, resulting in porosity and permeability deterioration, coal crushing, formation of fine coal and pulverized coal, seepage resistance enhancement and other issues. It will slow down the propagation of pressure drop (Palmer and Mansoori, 1998; Teyssedou et al., 2005; Li et al., 2009; Salmachi and Karacan, 2017; Yarmohammadtooski et al., 2017). The seam permeability, porosity and compression coefficient as well as the water drainage time would have high influences to the pressure drop speed at each point in the seam. The pressure drop would be positively related to the water drainage value, effective thickness of the seam, permeable rate of the seam, porosity, gas drainage time and water content of seam. The seam permeable rate, porosity and gas drainage time would be positively related to the pressure drop transmission distance in seam (Palmer, 2009). The larger the initial permeability in a certain direction, the smaller the absolute value of stress sensitivity coefficient, and the larger the control range of a single well is. The effect of stress sensitivity on the permeability of CBM reservoir and proposed production prediction method considering the stress sensitivity was evaluated (Meng et al., 2014). The ratio of drainage radius to producing pressure drop was adopted to classify and describe the shape of pressure drop funnel of homogeneous CBM reservoir, which also can be used to study the influence of permeability of coal reservoir, hydrodynamic conditions of reservoir, drainage, pressure drop funnel superposition on the shape of pressure drop funnel (Ibrahim et al., 2015).

However, there are few studies on the propagation velocity of pressure drop funnel and its sensitivity to reservoir physical parameters (McKee et al., 1998). This study focuses on the characteristics and influencing factors of the propagation velocity of pressure drop funnel in the stage of drainage and pressure reduction. The seepage equation of single-phase water in coal reservoir was modeled and solved numerically by using the software, COMSOL Multiphysics. The outer boundary conditions were set to be the constant pressure boundary, and the internal boundary condition was discussed according to the fixed bottomhole pressure and the constant speed drop of bottomhole pressure. On this basis, the influence of the initial porosity ( $\phi_0$ ), the initial permeability ( $k_0$ ), the elastic modulus ( $E$ ) and the Poisson ratio ( $\nu$ ) on the pressure drop transmission

was quantitatively studied.

## 2. Background of CBM well ZS39

The well used for pressure drop simulation in the single-phase water should be selected from the wells with lower critical desorption pressures. In this way, the adsorbed coalbed methane is not easy to desorb, which can ensure that the percolation is single-phase water. Data show that there is a fault communication aquifer and coal seam at the well ZS39 located in the southeast of the block, and the water content of the coal seam is extremely high. The critical desorption pressure of the coal seam is 0.147 MPa, and the original pressure of the reservoir is 10.60 MPa. The well ZS39 selected for simulation of pressure drop of single-phase water can set a lower bottomhole pressure, therefore there is a wide range of bottomhole pressures, and within these ranges the coalbed methane will not desorb.

## 3. Governing equations and solution method

Drainage and depressurization will increase the effective stress of the coal reservoir, cause the coal rock to undergo significant elastic-plastic deformation, and the pore and seepage space of the reservoir will be compacted or even closed, the permeability will decrease, showing the stress sensitive effect. The seepage equation of single-phase water in coal reservoir was derived considering the stress sensitivity.

### 3.1 Permeability model

Seidle et al. (1992) have studied the model that effective stress has an exponential effect on permeability. The model is based on a large number of rock mechanics experiments. This equation can be formulated as:

$$k = k_0 \exp(-3c_f(\sigma - \sigma_0)) \quad (1)$$

where  $\sigma$  is the effective stress (MPa);  $\sigma_0$  is the initial effective stress (MPa);  $k_0$  is the initial fracture permeability (mD);  $c_f$  is the fracture volume compression coefficient (1/MPa).

According to the stress-strain relationship model proposed by Moore (2012), the expression of the effective stress change neglecting the matrix shrinkage term in the equation is:

$$\sigma - \sigma_0 = -\frac{\nu}{1 - \nu}(p - p_0) \quad (2)$$

where  $p$  is the pore fluid pressure (MPa);  $p_0$  is the initial pore fluid pressure (MPa);  $\nu$  is Poisson ratio.

The expression of permeability change can be obtained by substituting Eq. (2) into Eq. (1) in the exponential relationship between coal permeability and effective stress. This equation can be formulated as:

$$k = k_0 \exp\left(3c_f \frac{\nu(p - p_0)}{1 - \nu}\right) \quad (3)$$

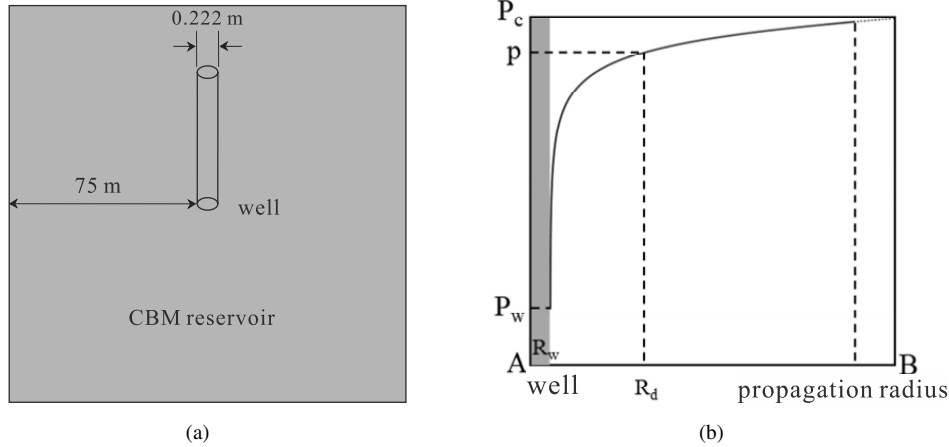


Fig. 1. The geometry mode of coalbed methane reservoir.

### 3.2 Porosity model

The classical cubic relationship between porosity and permeability derived from Kozeny-Carman equation is used as the porosity model (McKee et al., 1988):

$$k/k_0 = (\phi_f/\phi_{f0})^3 \quad (4)$$

The porosity model can be obtained by substituting Eq. (3) into Eq. (4):

$$\phi_f = \phi_{f0} \exp\left(c_f \frac{v(p-p_0)}{1-v}\right) \quad (5)$$

where  $\phi_f$  and  $\phi_{f0}$  are fracture porosity and its initial values.

### 3.3 Single phase water seepage model

In the more conventional Cartesian coordinate system, the continuity equation of single-phase water in the reservoir can be derived from the law of conservation of mass.

$$\frac{\partial(\rho u_x)}{\partial x} + \frac{\partial(\rho u_y)}{\partial y} = -\frac{\partial(\rho\phi)}{\partial t} \quad (6)$$

where  $\rho$  is the density of coal seam water ( $\text{kg/m}^3$ );  $u_i$  is the velocity in  $i$  direction ( $\text{m/s}$ );  $\phi$  is the porosity;  $t$  is time ( $\text{s}$ ).

The coal seam water is regarded as an incompressible fluid, so the density  $\rho$  at both ends of Eq. (6) can be directly reduced, so the equation become Eq. (7):

$$\frac{\partial u_x}{\partial x} + \frac{\partial u_y}{\partial y} = -\frac{\partial\phi}{\partial t} \frac{\partial p}{\partial t} \quad (7)$$

The seepage of coal seam water can be described by Darcy law:

$$u_i = -\frac{k}{\mu} \frac{\partial p}{\partial i} \quad (8)$$

where  $k$  is permeability ( $\text{m}^2$ );  $\mu$  is viscosity ( $\text{Pa}\cdot\text{s}$ );  $\partial p/\partial i$  is pressure gradient in  $i$  direction ( $\text{Pa/m}$ ). Substituting Eq. (8) into Eq. (7) can get Eq. (9):

$$\frac{\partial^2 p}{\partial x^2} + \frac{\partial^2 p}{\partial y^2} = \frac{\mu}{k} \frac{\partial\phi}{\partial p} \frac{\partial p}{\partial t} \quad (9)$$

The expression of fracture compression coefficient obtained by Mazumder et al. (2012) is considered, which does not take into account the matrix shrinkage effect caused by the compression of coal particles and gas desorption:

$$c_f = \frac{(1+v)(1-2\nu)}{(1-\nu)\phi_{f0}E} \quad (10)$$

where  $E$  is modulus of elasticity ( $1/\text{MPa}$ ).

By substituting the porosity and permeability model into Eq. (9), and replacing the fracture compression coefficient in the porosity and permeability model with Eq. (10), the control equation of single-phase water seepage in coal reservoir considering the stress sensitivity is obtained as follows:

$$\left[ \frac{\mu\alpha}{k_0E} \exp\left(\frac{-2\alpha(p-p_0)}{\phi_0E}\right) \right] \frac{\partial p}{\partial t} - \nabla^2 p = 0 \quad (11)$$

where

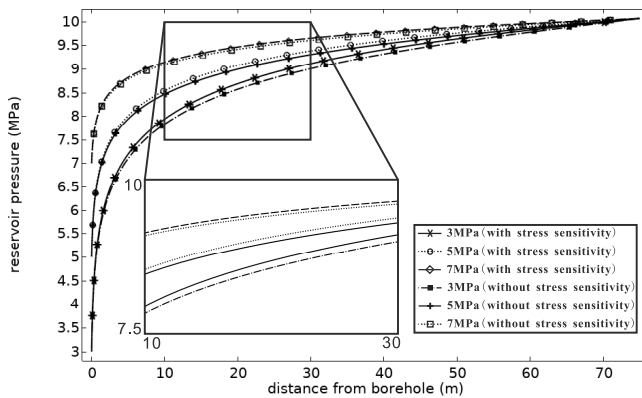
$$\alpha = \frac{(1+v)(1-2\nu)v}{(1-\nu)^2}$$

The above equation characterizes the seepage mode of single-phase water in coal reservoir. After the definite solution conditions are determined according to the specific simulation needs, the distribution rule of reservoir pressure can be solved by software calculation. In the actual simulation operation, the coefficient partial differential equation module in the numerical simulation software of COMSOL multiphysics is used. Boundary conditions can be set through the initial value and Dirichlet boundary conditions.

The geometry of coalbed methane reservoir with side length of 150 m and borehole with radius of 0.111 m are constructed (Fig. 1). Time data column set to start from day 1 and the time step is one day. The relevant parameters of ZS39 well are shown in Table 1.

**Table 1.** Parameters used in the simulation.

Parameters	Values	Data sources
Initial porosity ( $\phi_0$ )	0.03	Well testing
Poisson ratio ( $\nu$ )	0.33	Mechanics testing
Initial reservoir pressure ( $p_0$ , MPa)	10.06	Well testing
Initial permeability ( $k_0$ , $10^{-15}\text{m}^2$ )	0.094	Well testing
Formation water viscosity ( $\mu$ , mPa-s)	0.98	Well testing
Wellbore radius ( $r_w$ , m)	0.111	Well testing
Well control radius ( $r_e$ , m)	75	Empirical analogy
Elastic modulus ( $E$ , MPa)	210	Mechanics testing

**Fig. 2.** Comparison of reservoir pressure distribution of two types of coal reservoirs.

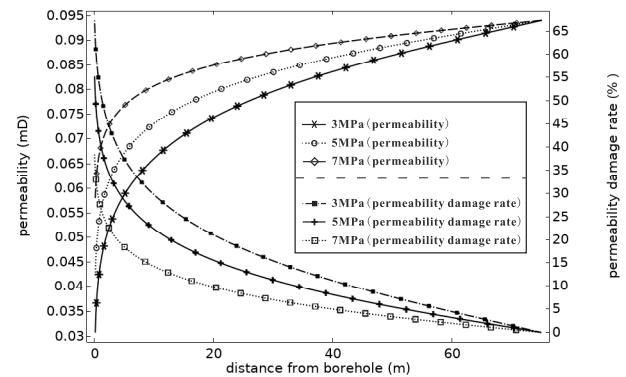
## 4. Results and discussions

### 4.1 Effect of stress sensitivity on pressure drop propagation

In order to evaluate the effect of stress sensitivity on the pressure drop propagation, the pressure drop propagation was simulated in reservoirs with and without considering stress sensitivity. Eq. (11) was used for the case where stress sensitivity is considered. And for the case where stress sensitivity is not considered, the most classical seepage control equation is used. Bottomhole pressure was set as 3 MPa, 5 MPa and 7 MPa. The radial distribution of reservoir pressure at the 500th day of drainage is shown in Fig. 2.

In the mode of constant pressure drainage, regardless of the bottomhole pressure, the pressure drop funnel in the deformed reservoir with stress sensitivity is always smaller than that of the non-deformed reservoir without stress sensitivity. The decrease of porosity and permeability caused by stress sensitivity obviously impedes the propagation of pressure drop funnel.

The influence of stress sensitivity on reservoir pressure drop is controlled by two main factors: bottomhole pressure and drainage time. Fig. 2 shows that after the same 500 days' drainage, the difference between the two types of pressure drop funnels will increase with the decrease of bottomhole pressure. When the bottomhole pressure is 7 MPa, the two

**Fig. 3.** Radial distribution of permeability and its damage rate.

curves almost coincide, and the difference between the two types of pressure drop funnels is not obvious. However, when the bottomhole pressure is 5 MPa and 3 MPa, the funnel gap becomes larger and larger.

Permeability damage ratio is used to evaluate permeability change. Permeability damage ratio can be defined as:

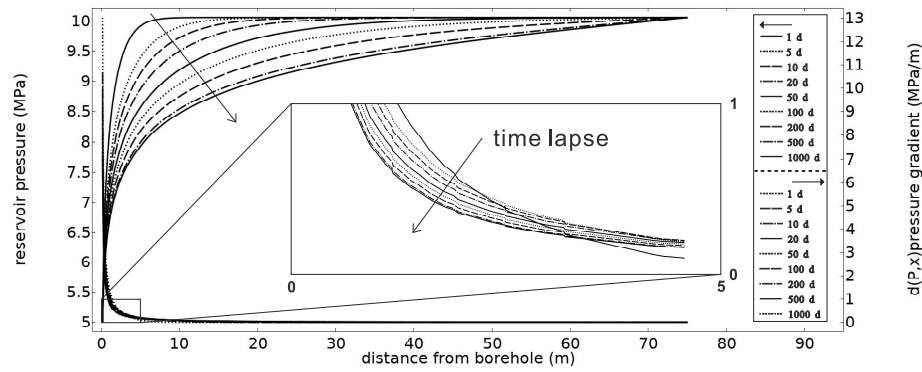
$$D = \frac{k_0 - k_n}{k_0} \times 100\% \quad (12)$$

where  $D$  is the damage rate of permeability (%);  $k_n$  is the permeability when the drainage pressure is reduced for  $n$  days (mD).

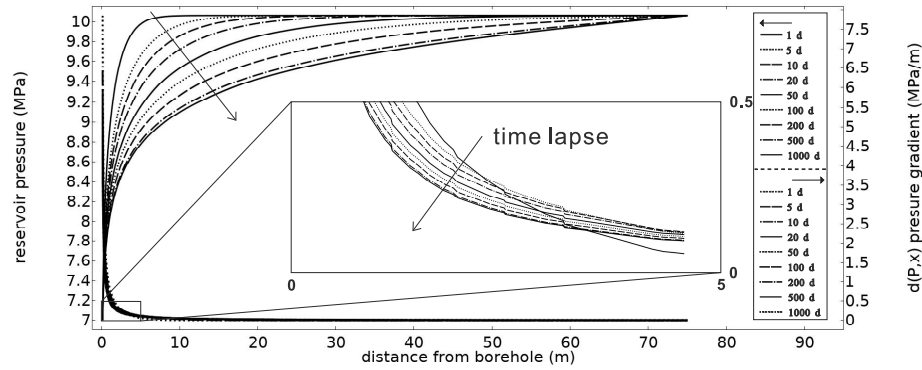
Furthermore, the radial distribution characteristics of permeability and permeability damage rate at the 1000th day with bottomhole pressure of 3 MPa, 5 MPa and 7 MPa were simulated. The results are shown in Fig. 3. Fig. 3 shows that the lower the bottomhole pressure is, the greater the permeability damage rate of the reservoir is. When the bottomhole pressure is 3 MPa, the permeability damage rate of the near well zone reaches more than 65%. This is because the premature and too fast drop leads to a great drop in permeability in the early stage.

### 4.2 Characteristics of pressure drop propagation

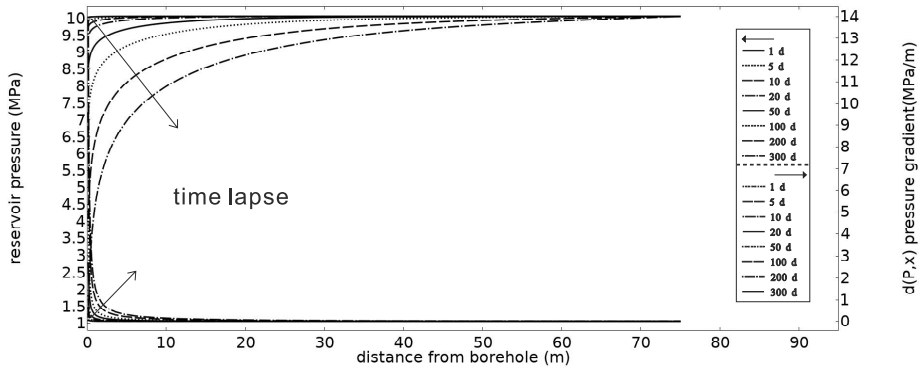
The propagation of pressure drop with fixed bottomhole pressure of 5 MPa, 7 MPa and constant pressure drop rate of



(a)



(b)



(c)

**Fig. 4.** Radial distribution characteristics of reservoir pressure and pressure gradient (a: Fixed bottomhole pressure: 5 MPa; b: Fixed bottomhole pressure: 7 MPa; c: Pressure drop at the speed of 0.03 MPa/d).

0.03 MPa/d were simulated. The radial distribution characteristics of reservoir pressure and pressure gradient in different drainage days are shown in Fig. 4(a), (b) and (c), respectively.

In the longitudinal direction, when the bottomhole pressure is fixed, the propagation rate of the pressure drop funnel slows down, and when the bottomhole pressure is lower, the propagation range of the pressure drop funnel is wider.

This is because the pressure gradient at the initial stage of drainage is large, and the stress sensitivity is not obvious, and the permeability has not been greatly damaged. As the drainage process goes on, the pressure drop funnel is further deepened in the longitudinal direction. Fig. 4(a) and (b) shows

that the pressure gradient near the well spacing is gradually decreased in the longitudinal direction; at the same time, due to the increase of stress sensitivity, the permeability of coal reservoir becomes poor, which makes the pressure drop more slowly.

While the pressure drop rate of the constant speed pressure drop mode in the longitudinal direction shows an increasing trend. Fig. 4(c) exhibits that in each radial position, the pressure gradient increases gradually with time lapse, but the decrease of porosity and permeability under the stress sensitive effect has a certain inhibition effect on the pressure drop, so the pressure drop rate increases slowly.



In the lateral direction, Fig. 4 shows that the pressure gradient decreases rapidly with the increase of the distance from the wellbore. Under the control of the radial distribution characteristics of the pressure gradient, the propagation of the pressure drop funnels in the two modes presents a significant deceleration trend.

In order to make the two modes comparable, the speed of the constant speed pressure drop mode was set to make the average pressure is 7 MPa in the beginning 28 days (the time pressure drop propagates to the boundary on the condition that bottomhole pressure is 7 MPa). i.e. 0.21857 MPa/d. The results are shown in Fig. 5.

In general, the lateral propagation rate of pressure drop funnel with constant bottomhole pressure is slightly higher than that with a steady decreasing in the pressure. However, when both of them spread to the boundary in about 30 days, the bottomhole pressure under the constant speed pressure drop mode has been reduced to a low pressure of 3.5 MPa. According to the previous analysis, the constant speed pressure drop mode will cause serious damage to the reservoir near the well zone. Therefore, in the actual process of drainage and depressurization, we can't blindly pursue to increase the production pressure drop. We should adopt the method of reducing the bottomhole pressure to the target value first and then adjusting it to a constant bottomhole pressure. In this way, we can expand the drainage radius as much as possible, the reservoir pressure drop can be fully expanded.

At the same time, in the process of fitting the relationship between the propagation distance and time of the pressure drop funnel, it is found that there is a very good power relationship between the propagation distance and time in the early stage (Fig. 5).

The pressure drop funnel index (PDFSI) was introduced as a comprehensive index to measure the scale of pressure drop funnel on day  $n$ , and its expression is as follows:

$$\text{PDFSI on day } n = \left( 1 - \frac{\int_{r_w}^{r_e} p_n dr}{p_i (r_e - r_w)} \right) \times 100\% \quad (13)$$

where  $p_i$  is the initial pressure of the reservoir (MPa);  $r_e$  and  $r_w$  are the well control radius and wellbore radius (m);  $p_n$  is the reservoir pressure on day  $n$  (MPa).

The pressure drop funnel index was used to quantify the characteristics of the pressure drop funnel propagation when the bottomhole pressure is 5 MPa and 7 MPa, and the two models used to study the lateral pressure drop propagation rate are compared. The results are shown in Fig. 6(a) and (b).

Due to the strong fluid-solid coupling characteristics of coal reservoir, the permeability and pressure of the reservoir are constantly changing, but they can reach a very close stable state when the permeability and pressure gradient are very small and almost constant in the late stage of drainage.

Fig. 6(a) shows that the scale of the funnel formed when the bottomhole pressure is 5 MPa is much larger than when the bottomhole pressure is 7 MPa through the same drainage time. Moreover, it can be found that the time for drainage to

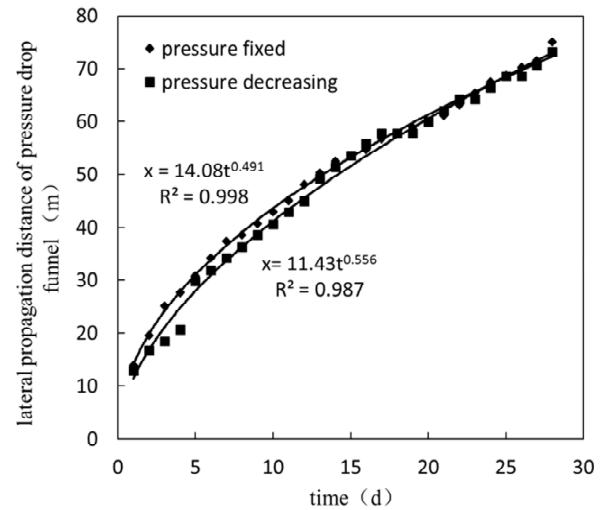


Fig. 5. Comparison of lateral spreading of pressure drop funnel.

reach near steady state is longer under lower bottomhole pressure. When the bottomhole pressure is 5 MPa and 7 MPa for drainage, the reservoir pressure reaches near steady state at about 1400 d and 1050 d, respectively.

In the comparison of the two modes, Fig. 6(b) indicates that the pressure drop propagation rate of the fixed bottomhole pressure increases rapidly at the initial stage and then decreases rapidly, which is quickly reversed by the pressure drop rate of the constant speed pressure drop mode. However, when the bottomhole pressure decreases at a constant speed, the pressure drop propagation rate is increasing all the time. This is because the continuous decrease of bottomhole pressure leads to the acceleration of longitudinal propagation of pressure drop funnel near the wellbore. It makes up for the deceleration of propagation of pressure drop funnel in the lateral direction, and the overall scale of pressure drop funnel shows the trend of acceleration.

### 4.3 Influence of physical parameters on pressure drop propagation

Different from the drainage pattern, the physical characteristics of coal reservoir itself can determine the pressure drop propagation from the mechanism. The physical parameters in Eq. (11) will affect the whole pressure drop process. In this section, based on the general law of pressure drop propagation in coal reservoirs, the sensitivity of pressure drop propagation to reservoir physical parameters was further simulated and studied.

According to Eq. (11), these parameters include  $\phi_0$ ,  $k_0$ ,  $E$  and  $\nu$ . We set other parameters as constant values, assigned different values to the reservoir physical parameters to be studied, and set the bottomhole pressure as 5 MPa constant pressure. The propagation process of pressure drop under each value was simulated.

Kept other physical parameters unchanged, set  $\phi_0$ ,  $k_0$ ,  $E$  and  $\nu$  as the data columns in Table 2.

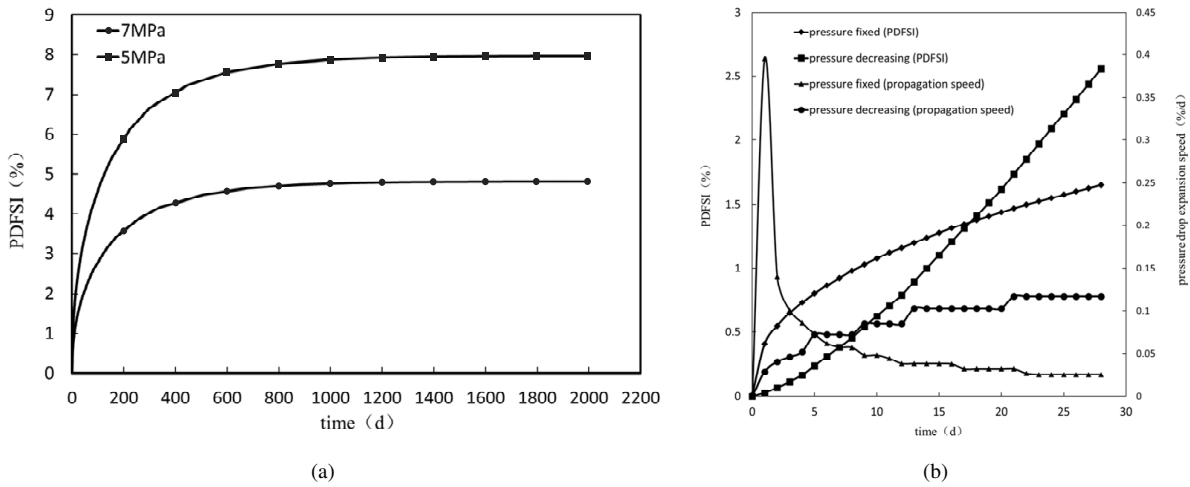


Fig. 6. PDFSI and propagation speed of PDFSI with time-variation.

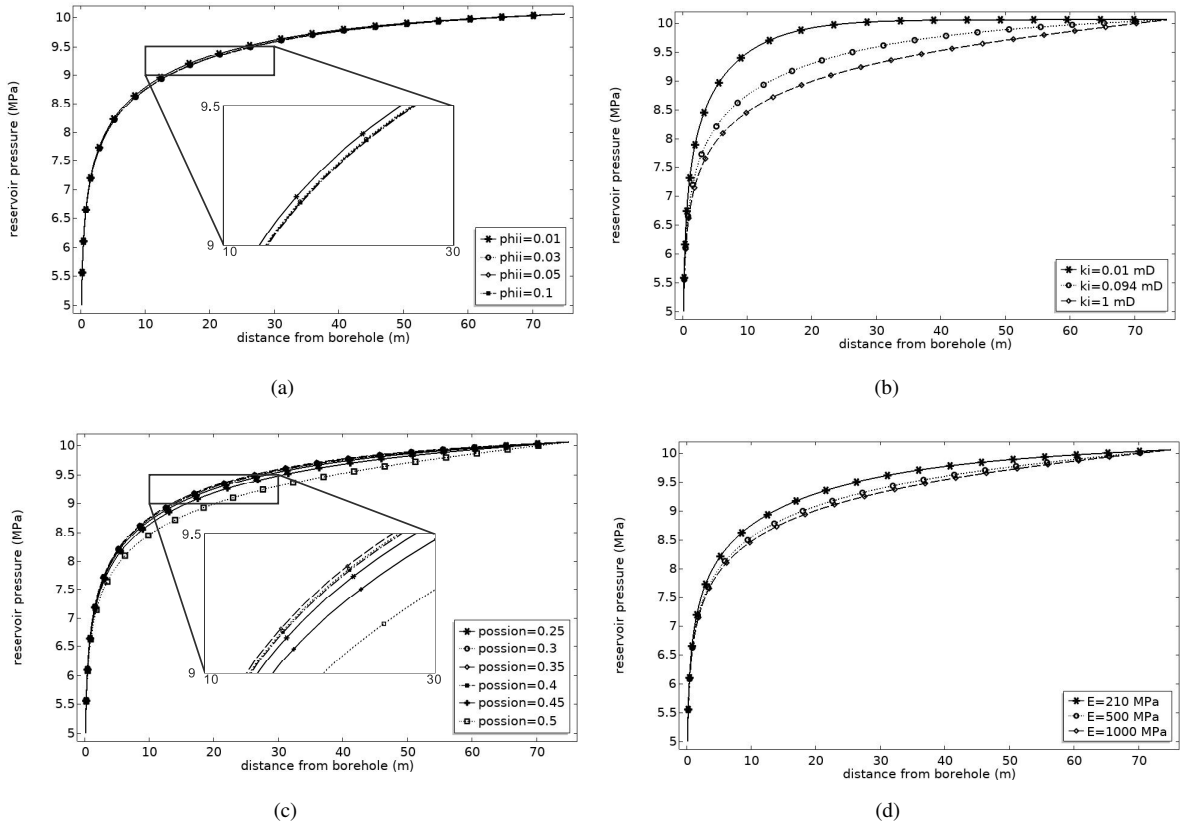


Fig. 7. Sensitivity of pressure drop to physical parameters.

Table 2. Physical parameter values of the numerical simulation.

Physical parameters	Values
$\phi_0$	phii=[0.01, 0.03, 0.05, 0.10]
$k_0$ (mD)	ki=[0.01, 0.094, 1]
$\nu$	posion=[0.25, 0.3, 0.35, 0.4, 0.45, 0.5]
$E$ (MPa)	E=[210, 500, 1000]

The simulation time was 200 days. The simulation results of different  $\phi_0$ ,  $k_0$ ,  $E$  and  $\nu$  are shown in Fig. 7 (a), (b), (c) and (d).

At the same time of drainage and production, the pressure drop funnel formed by the reservoir with larger initial porosity and permeability is larger. The initial porosity and permeability represent the fluid seepage space and capacity before deformation of the reservoir. Therefore, the larger these two parameters, the farther the pressure drop propagates.

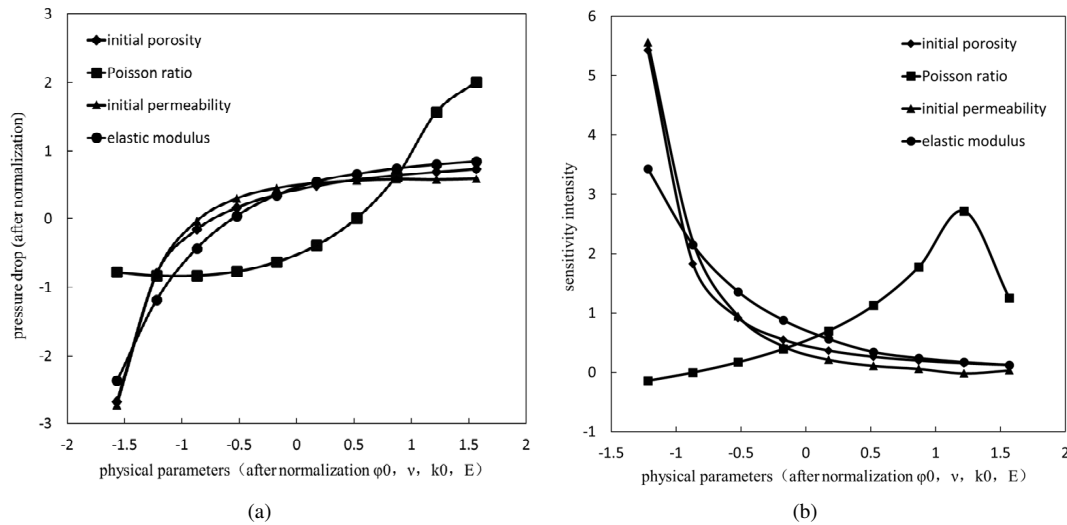


Fig. 8. Sensitivity of pressure drop to various parameter values.

Table 3. Physical parameter series.

Physical parameters	Values
$\phi_0$	range (0.1, 0.1, 1)
$k_0$ (mD)	range (0.1, 0.1, 1)
$\nu$	range (0.32, 0.02, 0.5)
$E$ (MPa)	range(210, 100, 1110)

Note: range (start, step, end).

In the process of drainage and depressurization of coal reservoir, the pressure of overlying strata on the coal reservoir is almost constant. With the discharge of coal seam water from the pores of coal seam, the effective stress on the coal rock skeleton increases, but at the same time, because the coal seam is confined in the horizontal direction, it is unable to extend in a large scale in the horizontal direction. Therefore, the lateral extension is transformed into the form of compression or even closure of larger seepage channels such as cleat fracture system, so the permeability will be reduced. However, when Poisson ratio continues to increase, the propagation range of pressure drop funnel will increase. This is because when Poisson ratio is large, the propagation trend of coal and rock is great in the horizontal direction, so the reservoir is greatly restricted in the horizontal direction. This makes the reservoir unable to be extended enough in the transverse direction even if it has a large seepage hole fracture compression. In this way, due to the surrounding rock confining force, it has a resistance effect on the vertical compression, which makes the effective stress effect weaken, so the propagation scale of pressure drop funnel is larger. For the elastic modulus, the larger the elastic modulus is, the larger the pressure drop funnel is. Because the elastic modulus can represent the firmness of coal rock, the larger the elastic modulus is, the less easy it is to deform. Therefore, the larger the value, the smaller the damage of permeability. And the pressure drop funnel is larger.

To quantitatively describe the sensitivity of reservoir pressure drop to different physical properties, a series of different values were given to the above physical parameters based on the actual situation of the coal reservoir as detailed listed in Table 3.

Taking the above values, the pressure drop at a distance of 20 m from the borehole was simulated. The simulation results are normalized (Fig. 8(a)), and the derivative is used as a measure of sensitivity intensity, as shown in Fig. 8(b).

When the value of physical parameters is low ( $\phi_0$  is less than 0.3,  $k_0$  is less than 0.3 mD,  $E$  is less than 400 MPa,  $\nu$  is less than 0.35), the sensitivity of pressure drop to porosity and permeability is strong, followed by modulus of elasticity, and the pressure drop is positively related to these three parameters. While the sensitivity to Poisson ratio is weak, and the pressure drop is negatively correlated. With the increase of each parameter value, the sensitivity of pressure drop to both porosity and modulus of elasticity decreases, but the sensitivity to modulus of elasticity gradually exceeds the sensitivity to porosity and permeability, and the sensitivity of pressure drop tends to 0 when  $\phi_0$  is close to 1,  $k_0$  is close to 1 mD,  $E$  is close to 1200 MPa, which indicates that when these physical conditions reach the above very ideal conditions, the propagating of pressure drop funnel is very fast, reaching stable at 200 days, while the pressure drop becomes positive correlation with Poisson ratio, and the sensitivity is increasing.

## 5. Conclusions

The propagation velocity of pressure drop funnel and its sensitivity to reservoir physical parameters were studied using numerical simulation. The effect of the  $\phi_0$ ,  $k_0$ ,  $E$  and  $\nu$ , on the pressure drop funnel was investigated. The following conclusion can be drawn from this study:

- 1) Compared with the pressure drop propagation without considering the stress sensitivity, when considering the stress sensitivity, the permeability will form a permeability drop funnel with the same shape as the pressure drop



funnel, which will cause serious damage to the reservoir near the wellbore.

- 2) Under the condition of fixed bottomhole pressure, the propagation rate of reservoir pressure drop funnel decreases gradually in both vertical and horizontal directions, and the overall propagation rate increases rapidly first and then decreases gradually; When the bottomhole pressure drops at a constant speed, the pressure drop rate increases in the vertical direction and decreases in the horizontal direction. The overall propagation speed of the pressure drop funnel increases with time.
- 3) The propagation of pressure drop is positively correlated with  $\phi_0$ ,  $k_0$  and  $E$ , and the sensitivity decreases with the increase of these three physical parameters; when  $v$  is small, the propagation of pressure drop is negatively correlated with it, and becomes positive correlation with the increase of  $v$ , the sensitivity increases gradually at the same time.

## Acknowledgments

This research was funded by the Fundamental Research Funds for Central Universities (Grant No. 2652018002)

**Open Access** This article is distributed under the terms and conditions of the Creative Commons Attribution (CC BY-NC-ND) license, which permits unrestricted use, distribution, and reproduction in any medium, provided the original work is properly cited.

## References

- Adusu, P.T. Optimising candidate well selection for matrix stimulation-IPR approach. Paper SPE 198707 Presented at SPE Nigeria Annual International Conference and Exhibition, Lagos, Nigeria, 5-7 August, 2019.
- Clarkson, C.R. Case study: Production data and pressure transient analysis of Horseshoe Canyon CBM wells. *J. Can. Petrol. Technol.* 2009, 48(10): 27-38.
- Clarkson, C.R., Qanbari, F. A semi-analytical method for forecasting wells completed in low permeability, undersaturated CBM reservoirs. *J. Nat. Gas Sci. Eng.* 2016, 30: 19-27.
- Connell, L.D. A new interpretation of the response of coal permeability to changes in pore pressure, stress and matrix shrinkage. *Int. J. Coal Geol.* 2016, 162: 169-182.
- Dejam, M., Hassanzadeh, H., Chen, Z. Semi-analytical solution for pressure transient analysis of a hydraulically fractured vertical well in a bounded dual-porosity reservoir. *J. Hydrol.* 2018, 565: 289-301.
- Hu, H., Jin, J., Zhao, L., et al. Effects of pressure drop funnels model of different shapes on CBM well productivity. *Coal Geol. Explor.* 2019, 47(3): 109-116 (in Chinese).
- Ibrahim, A.F., Nasr-El-Din, H.A. A comprehensive model to history match and predict gas/water production from coal seams. *Int. J. Coal Geol.* 2015, 146: 79-90.
- Ide, T.S., Pollard, D., Orr, F.M. Fissure formation and subsurface subsidence in a coalbed fire. *Int. J. Rock Mech. Min. Sci.* 2010, 47(1): 81-93.
- Li, J., Su, X., Lin, X. Relationship between discharge rate and productivity of coalbed methane wells. *J. China Coal Soc.* 2009, 34(3): 376-380 (in Chinese).
- Liu, Y., Lou, J. Study on reservoir characteristics and development technology of coalbed gas in China. *Nat. Gas Ind.* 2004, 24(1): 68-71 (in Chinese).
- Majdi, A., Hassani, F.P., Nasiri, M.Y. Prediction of the height of destressed zone above the mined panel roof in longwall coal mining. *Int. J. Coal Geology.* 2012, 98: 62-72.
- Mazumder, S., Scott, M., Jiang, J. Permeability increase in Bowen Basin coal as a result of matrix shrinkage during primary depletion. *Int. J. Coal Geol.* 2012, 96: 109-119.
- McKee, C.R., Bumb, A.C., Koenig, R.A. Stress-dependent permeability and porosity of coal and other geologic formations. *SPE Form. Eval.* 1988, 3(1): 81-91.
- Mendhe, V.A., Kamble, A.D., Bannerjee, M., et al. Evaluation of shale gas reservoir in Barakar and barren measures formations of north and south Karanpura Coalfields, Jharkhand. *J. Geol. Soc. India.* 2016, 88(3): 305-316.
- Meng, Z., Zhang J., Liu, H., et al. Productivity model of CBM wells considering the stress sensitivity and its application analysis. *J. China Coal Soc.* 2014, 39(4): 593-599 (in Chinese).
- Moore, T.A. Coalbed methane: A review. *Int. J. Coal Geol.* 2012, 101: 36-81.
- Palmer, I., Mansoori, J. How permeability depends on stress and pore pressure in coalbeds: A new model. *SPE Reserv. Eval. Eng.* 1998, 1(6): 539-544.
- Palmer, I. Permeability changes in coal: Analytical modelling. *Int. J. Coal Geol.* 2009, 77: 119-126.
- Salmachi, A., Karacan, C.Ö. Cross-formational flow of water into coalbed methane reservoirs: Controls on relative permeability curve shape and production profile. *Environ. Earth Sci.* 2017, 76(5): 200.
- Sang, S., Xu, H., Fang, L., et al. Stress relief coalbed methane drainage by surface vertical wells in China. *Int. J. Coal Geol.* 2010, 82(3): 196-203.
- Seidle, J., Jeansonne, M.W., Erickson, D.J. Application of matchstick geometry to stress dependent permeability in coals. Paper SPE 24361 Presented at SPE Rocky Mountain Regional Meeting, Casper, Wyoming, 18-21 May, 1992.
- Teyssedou, A., Onder, E.N., Tye, P. Airwater counter-current slug flow data in vertical-to-horizontal pipes containing orifice type obstructions. *Int. J. Multiph. Flow* 2005, 31(7): 771-792.
- Wang, C., Shao, X., Sun, Y., et al. Production decline types and their control factors in coalbed methane wells: A case from Jincheng and Hancheng mining areas. *Coal Geol. Explor.* 2013, 41(3): 23-28 (in Chinese).
- Wang Y., Wang C., Wang F. Analysis on the relationship between pressure drop laws and production parameters of CBM well: A case study on the Baode Block. *Oil Drill. Prod. Technol.* 2019, 41(4): 502-508.
- Yarmohammadtooski, Z., Salmachi, A., White, A., et al. Fluid flow characteristics of bandanna coal formation: A case study from the fairview field, eastern Australia. *Aust. J. Earth Sci.* 2017, 64: 319-333.